ADVANCED MATERIALS

Supporting Information

for *Adv. Mater.*, DOI: 10.1002/adma.201603507

Coding Acoustic Metasurfaces

Boyang Xie, Kun Tang, Hua Cheng, Zhengyou Liu, Shuqi Chen,* and Jianguo Tian**

Supporting Information

Coding acoustic metasurfaces

*Boyang Xie, Kun Tang, Hua Cheng *, Zhengyou Liu, Shuqi Chen *, and Jianguo Tian **

1. Theoretical Analysis for Producing the Coding Elements "0" and "1"

We first consider the periodic arranged Helmholtz resonator like structure, as shown in **Figure S1**a. The lowest dispersion band supported by the structure is shown in Fig. S1c. At the point of $k_x p/2\pi$ = 0.25, f = 4200 Hz, the phase difference between two unit cells is definitely π. This can be verified by analyzing two unit cells, as shown in Fig. S1b. If we test two unit cells by plane wave incidence at one end and probe at the other end, we can get the phase and transmission respond of the structure in Fig. S1d. The transmission shows strong local resonance. The resonant peak appear at f = 4200 Hz and the phase accumulation is π. The resonant frequency can also be simply estimated from the equivalent LC-circuit as $f = 1/2\pi\sqrt{MC}$, where $M = \rho_0 a/(H-2h-b)$ is the acoustic mass in the narrow gap, and $C = (p-a)(H-2h)/\rho_0 c_0^2$ is the acoustic capacitance of the space between two bumps. Therefore, the resonant frequency is determined by the local geometry inside the elements. For our design, as $H = L/5$, $a = L/15$, $b = L/10$, $p = L/6$, and $h = L/24$ for L = 6.2 cm, the resonant frequency given by the circuit model is 4212 Hz, which is in good agreement with the FEM simulation with 4200 Hz. We use two slit-cavities to couple the wave in/out of the local resonance. The two slit-cavities are connected directly for coding element "0", and connected to the left and right ends of a two-cavity resonant structure for coding element "1". Thus, the phase difference between the coding elements "0" and "1" is π. However, the

simulated resonant frequency of the elements “0” and “1” is shifted to 4453 Hz due to the structure coupling.

2. Multiplicity of Coding Elements of “0” and “1”

The coding elements of “0” and “1” mentioned in the main text are not the only choice. Although the metasurface unit cells with sub-wavelength cavities are sensitive to the position of slit, we can achieve the similar coding functionality by varying the number of the cavity or the positions of the slits. A_i and B_j (i, j =1, 2, 3, …) are used to represent the slit positions on the upper and lower plates of the coding elements, respectively. **Figure S2** shows the schematic diagram of coding elements with four and six cavities. By combination of A_i and B_i, all possible coding elements of “0” and “1” described in **Table S1** can still realize similar transmission spectrum with a phase difference close to π. The transmission and phase spectra of the coding element with four cavities are show in **Figure S3**. The transmission coefficient of the element “0” has a slight divergence from the element “1” in shorter wavelength as the resonance is interfered by other local modes. However, the coding elements with four cavities are good candidates for realizing the coding functionality with smaller size. The elements with cavity number less than four cannot realize the coding functionalities of “0” and “1” by changing the position of the slits. Similar coding functionalities of “0” and “1” can also be obtained at lower frequency for the elements with cavity number not less than eight, which will induce diffraction at the considered resonant frequency range.

3. Performances of the Coding Acoustic Metasurfaces in Different Wavelengths

As the phase difference can reach π in a certain wavelength range and the transmission amplitudes of coding elements “0” and “1” are superposed each other, the performances of the coding acoustic metasurfaces can be realized both numerically and experimentally in a certain wavelength range for one-dimensional (1D) coding test. We show the simulated and measured transmitted temporal field distributions with normally incident wave at the frequencies of 4350 Hz and 4650 Hz in **Figure S4**a-S4d, respectively. The corresponding

phase distributions are also plotted in **Figure S5**a-S5d. The incident wave is refracted into two branches. The wavefronts of diffractive orders are flat in the farfield, which are more recognizable in the phase distributions. These phenomena are obvious and overall in agreement with the theory. The performances of 1D Fresnel lens are also shown in **Figure S6**a-S6d for the frequencies of 4400 Hz and 4580 Hz. The focal point can be clearly observed from the simulated and measured results.

4. Fresnel Lens with short Focal Length by Coding along the Elongated Direction

The minimum focal length for the 1D Fresnel lens discussed in the main text cannot be shorter than 40 cm as the size of the outermost zone of 1D Fresnel lens must be greater than or equal to the coding unit length. For example, for the Fresnel lens with focal length of 13 cm, the simulated zone parameters should be r_1 = 10.2 cm, r_2 = 15.4 cm, r_3 = 20.0 cm, r_4 = 24.3 cm, and r_5 = 28.5 cm for successive five zones. The length of the outermost zone is of r_5 - r_4 = 42 mm, which is shorter than the coding unit length of L = 62 mm. Thus, the 1D Fresnel lens coding in the main text cannot be directly realized a short focal length. However, the geometric restriction of Fresnel lens can be ignored by coding along the elongated direction, as shown in **Figure S7**a. The simulated intensity profile for the focusing effect is given in Fig. S7b. The Fresnel lens with short focal length of 13 cm can be achieved according to the simulation. The Fresnel lens with shorter focal length can be further obtained with the decreasing of the zone parameters by means of coding along the elongated direction.

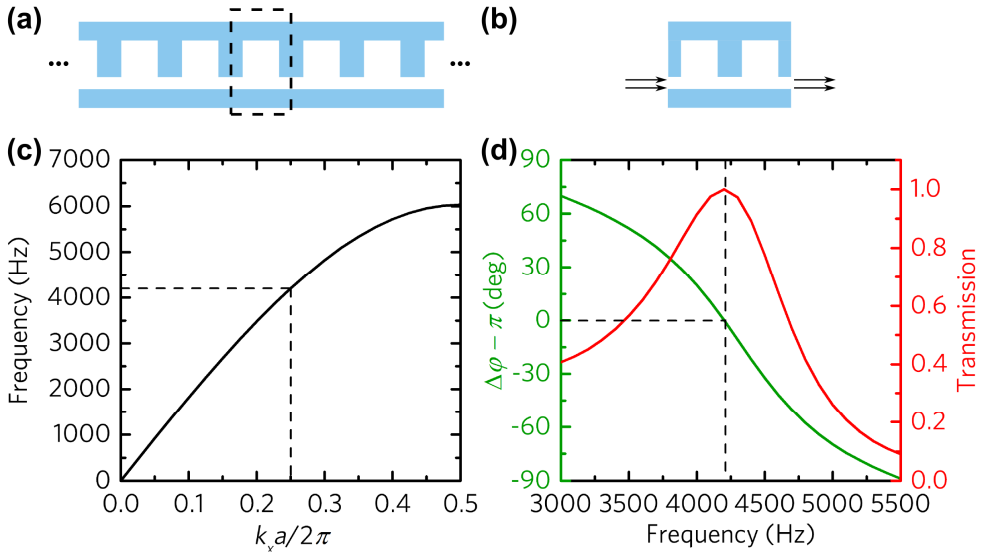

Figure S1 (a) The periodic arranged Helmholtz-like structure and (c) its first dispersion band. The dashed rectangular frame area represents its unit cell. (b) Two-cavity structure incident by plane wave and (d) its phase and transmission responds.

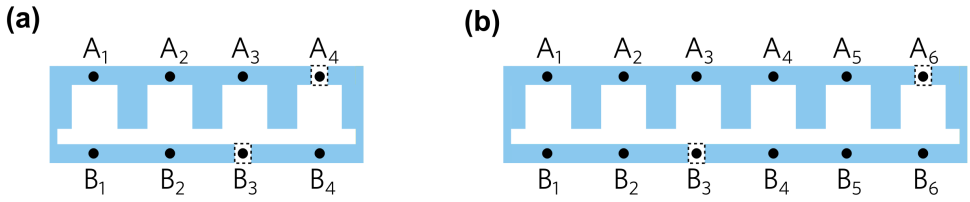

Figure S2. Schematic diagram of coding elements with (a) four and (b) six cavities. A_i and B_j (i, j = 1, 2, … , 6) are the positions of slits opened on the upper and lower plates. The slits are opened at A_4, A_6, and B_3 in the coding elements of (a) and (b).

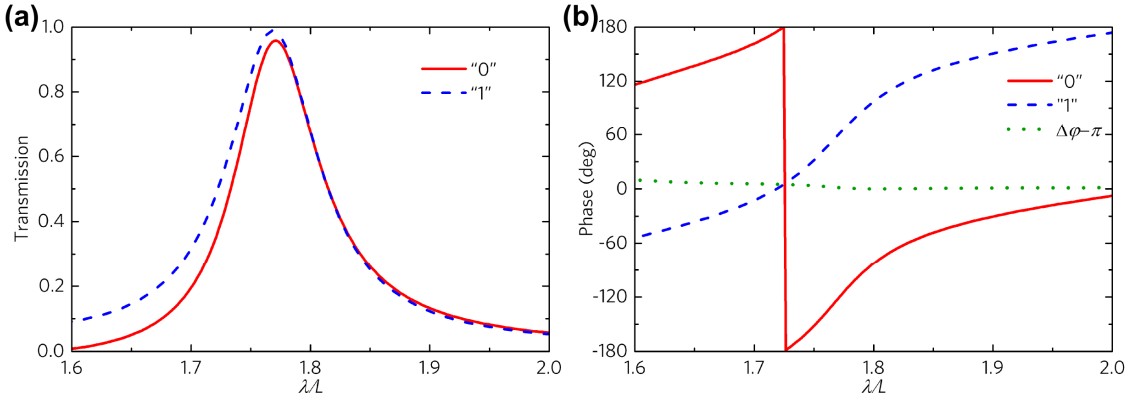

Figure S3. (a) Transmission amplitude and (b) phase of acoustic waves transmitting through the four-cavity coding elements of "0" and "1".

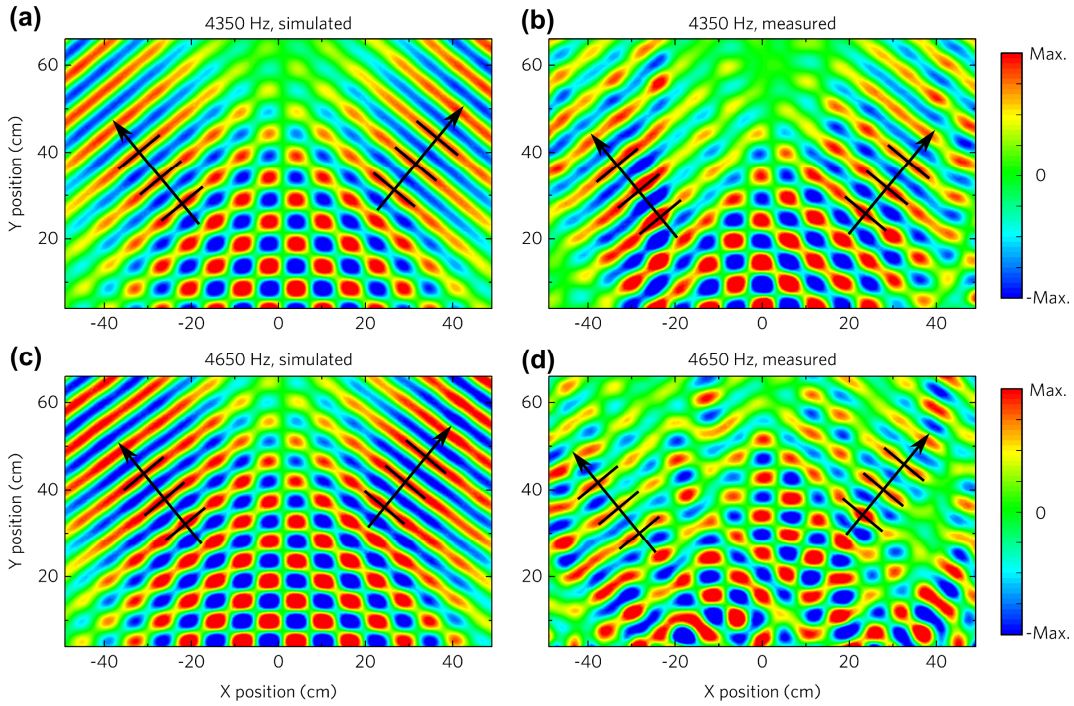

Figure S4. (a), (c) Simulated and (b), (d) measured acoustic temporal field distributions of the transmitted waves at the frequencies of 4350 Hz and 4650 Hz, which are normally incident on the coding acoustic metasurface.

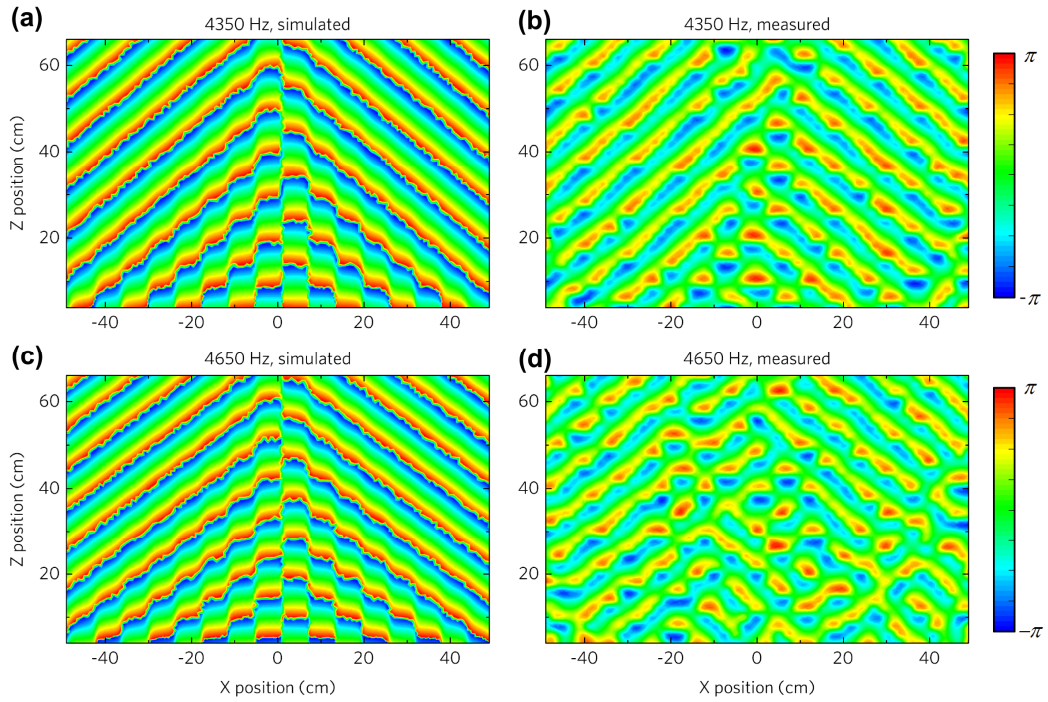

Figure S5. (a), (c) Simulated and (b), (d) measured phase distributions of the transmitted waves at the frequencies of 4350 Hz and 4650 Hz, which are normally incident on the coding acoustic metasurface.

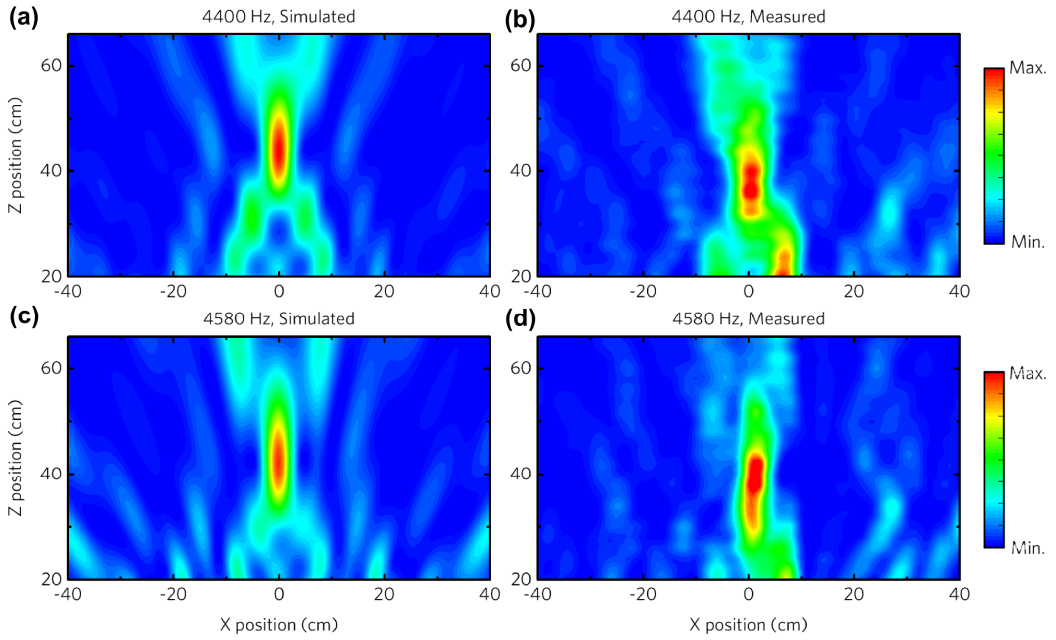

Figure S6. (a), (c) Simulated and (b), (d) measured intensity profile for the focusing effect at the frequencies of 4400 Hz and 4580 Hz.

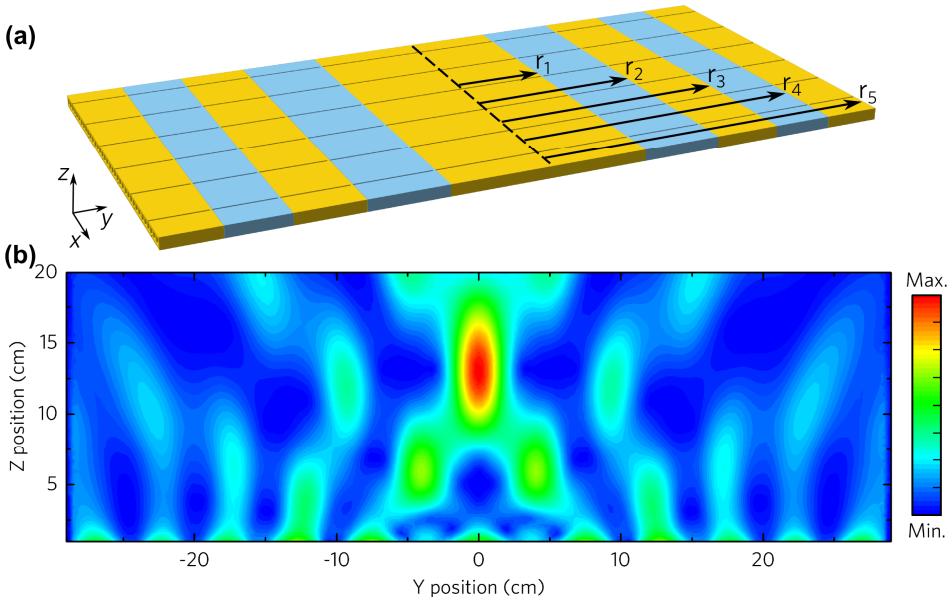

Figure S7. (a) Schematic diagram for the designed Fresnel lens. (b) Simulated intensity profile for the designed Fresnel lens with short focal length.

Number of cavity	Element "0"	Element "1"
Four	$A_1B_2(A_4B_3)$, $A_2B_1(A_3B_4)$	$A_1B_4(A_4B_1)$
Six	$A_1B_2(A_6B_5)$, $A_2B_1(A_5B_6)$ $A_3B_4(A_4B_3)$, $A_1B_6(A_6B_1)$	$A_1B_4(A_6B_3)$, $A_3B_6(A_4B_1)$

Table S1. Possible coding elements of "0" and "1" with different slit positions.